ANKLE CARTILAGE SURFACE SEGMENTATION USING DIRECTIONAL GRADIENT VECTOR FLOW SNAKES

Jinshan Tang[+], Steven Millington[#], and Scott T. Acton[+], Jeff Crandall[*] and Shepard Hurwitz[#]*
[+]Department of Electrical Engineering,
*Center for Applied Biomechanics, [#]Department of Orthopaedic Surgery
University of Virginia, Charlottesville, VA 22903 USA

ABSTRACT

Ankle cartilage surface segmentation is a pre-step to compute the cartilage thickness which is used to evaluate the treatment of ankle joint diseases. Because of the un-ideal imaging condition, the acquired ankle images are often noised and the cartilage parts in the images are often disconnected, thus traditional techniques such as gradient-based edge detection are not suitable for the segmentation of these surfaces. In this paper, we developed an active contour model based ankle cartilage surface segmentation algorithm. The algorithm used gradient vector flow (GVF) as external forces. In order to make the GVF snake more stable and to converge at the correct surfaces, directional gradient is used to produce the gradient vector flow field. Experimental results indicate that the new approach utilizing directional gradient is more robust than the traditional GVF snake.

1. INTRODUCTION

Osteoarthritis is a common form of disability in the United States. According to estimation, the cost was approximately $65 billion per year during the 1990's [1]. This cost is only set to rise with an aging population and rising drug costs. The potential impact of chondro-protective treatments and articular cartilage restoration techniques are significant. Currently precise evaluation of a patients degenerative joint(s), qualitatively and quantitatively both pre- and post treatment is technically demanding, especially in highly congruent joints with thin articular cartilage, e.g., the ankle joint. However, in order to clinically evaluate present and future treatments, we must be able to precisely and reproducibly quantify the articular cartilage of these joints[2].

In order to quantify the articular cartilage of these joints, we need to extract/segment the surfaces of highly congruent joints with thin articular cartilage layers. The accuracy of the surface extraction and segmentation of highly congruent joints with thin articular cartilage layers can have a significant effect on the percentage errors and reproducibility of quantitative measurements (i.e. thickness and volume) of the articular cartilage.

Previous studies have performed segmentation using manual surface extraction and segmentation [3]. However, manual surface extraction and segmentation is both labor intensive, prone to error and subject to subjective judgment of an observer leading to inter-observer variability.

An appropriate algorithm for this application is the active contour model or snake [4], which usually is formulated using partial differential equations (PDEs). A snake is a parameterized contour [4] that translates and deforms on the image plane according to the strength of the image edges and the internal properties of the contour such as smoothness. Many active contour models have been proposed since the original active contour model was introduced by Kass *et al*. [4]. This paper adopts and modifies a GVF snake developed originally in [5]. The advantage of such a model is its robustness to the initialization of the snake [5]. Because the cartilage of the ankle is very thin and the surfaces are closely located, the current GVF snake model is not effective in the segmentation of the surface. We propose a GVF algorithm that exploits the edge direction information. This additional information makes the snake more stable and allows the snake to converge to the correct surfaces.

2. MATERIALS AND METHODS

2.1. Data collection

The MR images of the ankle were acquired using a 1.5 T MR scanner (Magneton vision, Siemens, Erlargen, Germany) and a circularly polarized transmit receive extremity coil. The imaging sequence used was a sagittal spoiled 3D gradient-echo sequence, fast low angle shot (FLASH), with selective water excitation, TR of 18 ms, TE of 7.65 ms, flip angle of 25°, in-plane resolution of 0.3 mm x 0.3 mm, slice thickness of 0.3 mm, and field of view 160 mm (512x512 pixels). The acquisition time required was 17 mins 14 secs. As the images were acquired using isotropic voxels image, we were able to reconstruct the images in three perpendicular planes

0-7803-8554-3/04/$20.00 ©2004 IEEE.

(sagittal, coronal and axial). All image data were then transferred to a desktop work station for surface extraction and segmentation.

2.2. Boundary Segmentation using Directional GVF Snake

2.2.1. GVF snake

Kass *et al*. [4] define a snake as a controlled continuity contour which is attracted to salient image features, such as edges by minimizing the following energy function.

$$E_{snake} = \int_0^1 [E_{\text{int}}(\mathbf{r}(s)) + E_{ext}(\mathbf{r}(s))]ds \quad (3)$$

where E_{int} and E_{ext} represent the internal energy and the external forces respectively. $\mathbf{r}(s) = (x(s), y(s))$ represents the position of a snake parametrically. The internal force keeps the active contour smooth and may be defined as [4]

$$E_{\text{int}} = (\alpha|\mathbf{r}_s(s)|^2 + \beta|\mathbf{r}_{ss}(s)|^2)/2 . \quad (4)$$

The external energy is application-based and is used for guiding the active contour toward the image features of interest, which is typically defined as $-|\nabla G_\sigma(x,y) * I(x,y)|$. The minimization problem of (3) leads to the following Euler equations

$$\alpha x_{ss} - \beta x_{ssss} - \frac{\partial E_{ext}}{\partial x} = 0 , \quad (5)$$

$$\alpha y_{ss} - \beta y_{ssss} - \frac{\partial E_{ext}}{\partial y} = 0 \quad (6)$$

From (5) and (6), we can obtain a discrete evolution equations as follows [3]

$$\mathbf{x}_t = (A + rI)^{-1}(r\mathbf{x}_t - f_{\mathbf{x}}(\mathbf{x}_{t-1}, \mathbf{y}_{t-1})) \quad (7)$$

$$\mathbf{y}_t = (A + rI)^{-1}(r\mathbf{y}_t - f_{\mathbf{x}}(\mathbf{x}_{t-1}, \mathbf{y}_{t-1})) \quad (8)$$

where r is a step size, $(\mathbf{x}_{t-1}, \mathbf{y}_{t-1})$ is the previous position of the snake and $(\mathbf{x}_t, \mathbf{y}_t)$ is the current position of the snake.

One of the disadvantages of the snake defined by (3) is the sensitivity to the initialization of the snake. The initial contour must be close to the actual object boundary because the capture range of the image gradient is small. To alleviate this problem, gradient vector flow (GVF) is proposed in [5] as an external force to attract the snake to actual boundary of the objects. GVF fields are computed by a diffusion process, which can be implemented by minimizing the following energy function [5]:

$$E_{\text{GVF}}(u,v) = \frac{1}{2}\iint \{\mu(u_x^2 + u_y^2 + v_x^2 + v_y^2) + |\nabla f|^2 (\mathbf{v} - \nabla f)^2\} dxdy \quad (9)$$

where μ is a regularization parameter governing the tradeoff between the first term and the second term in the integrand, and f is the edge map. When $|\nabla f|$ is small, the energy is dominated by the first term, yielding a slowly varying field, and when $|\nabla f|$ is large, the energy is dominated by the second term, which forces the vector solution to be close to the gradient near the edges. Variational minimization of (9) results in the following two Euler equations[5]:

$$\begin{aligned} \mu\nabla^2 u - (f_x^2 + f_y^2)(u - f_x) = 0, \\ \mu\nabla^2 v - (f_x^2 + f_y^2)(v - f_y) = 0. \end{aligned} \quad (10)$$

Solving (10) for (u,v) results in gradient vector flow (GVF) field that acts as an external force field for the active contour.

Replacing the external forces $(-\frac{\partial E_{ext}}{\partial x}, -\frac{\partial E_{ext}}{\partial y})$ (in the x and y directions, respectively) with a vector field (u, v), we have:

$$\alpha x_{ss} - \beta x_{ssss} + u(x(s), y(s)) = 0 , \quad (11)$$

$$\alpha y_{ss} - \beta y_{ssss} + v(x(s), y(s)) = 0 . \quad (12)$$

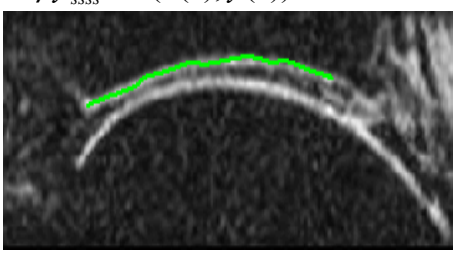

(a) Initialization of the snake

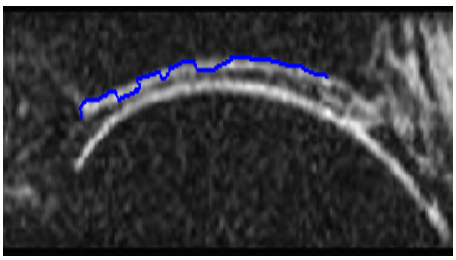

(b) Tracking results by GVF

Figure 1. Example of tracking results using the traditional GVF snake.

2.2.2. *Directional Gradient Vector Flow for boundary detection*

With the GVF snake, only the gradient magnitude is used to compute the gradient vector flow. Thus, the traditional GVF snake may be attracted to strong edges that have the opposite gradient direction with respect to the correct boundary. Figure 1 demonstrates this point. In Figure 1,

the image includes four boundaries (from top to bottom) corresponding to four surfaces: Tibial bone-cartilage interface, tibial cartilage surface, Talar cartilage surface and Talar bone-cartilage interface. We hope to capture the boundary corresponding to the Tibial bone-cartilage interface. If we initialize the snake as Figure 1(a), then we found that the some part of the snake converges to the boundary corresponding to Tibial bone-cartilage interface while the some part of the snake converges to the boundary corresponding to tibial cartilage surface. This means that GVF active contour fails to capture the boundary of the object we are looking for.

In order to utilize the edge direction information in the snake, we use the edge map function considering gradient direction information which is computed by

$$D_{\mathbf{n}}(I) = \nabla I \bullet \mathbf{n} \qquad (13)$$

where I is the original image, ∇I is the gradient and $\mathbf{n}$ is a two-dimensional vector which represents the direction of the edge, which can be specified by the user (and is known a priori for the ankle cartilage application).

Let

$$F = \begin{cases} D_n(I) & if \quad D_n(I) > 0 \\ 0 & others \end{cases} \qquad (14)$$

Replacing f by F in (9), we obtain the directional gradient vector flow (DGVF) of the image by minimizing the following equation

$$E_{GVF}(u,v) = \frac{1}{2}\iint \{\mu(u_x^2 + u_y^2 + v_x^2 + v_y^2) + |\nabla \mathbf{F}|^2 (\mathbf{v} - \nabla \mathbf{F})^2\} dxdy \qquad (15)$$

Figure 2(b) shows the gradient vector flow of the original image shown in Figure 2(a). Figure 2(c) shows the tracking results using traditional GVF snake (here we hope to capture the top boundary in the image). In Figure 2(c), the green curve is the initial curve, and the blue curve is the final contour. From Figure 2(c), it may be observed that the traditional snake failed to capture the top boundary because of the initialization. Figure 2 (d) shows that the enhanced directional gradient vector flow, and Figure 2(e) shows the tracking results using the directional GVF (DGVF) snake. Figure 2(e) demonstrates that the DGVF snake captures the boundary as intended. Figure 3 shows the tracking results using the initialization in Figure 2(a). Compared the tracking result obtained by traditional GVF snake Figure 2(b) and the Directional GVF snake, we can know that the use of direction information in the GVF model has cause the snake converge to the right surface (Tibial bone-cartilage interface).

(a) Original synthetic image

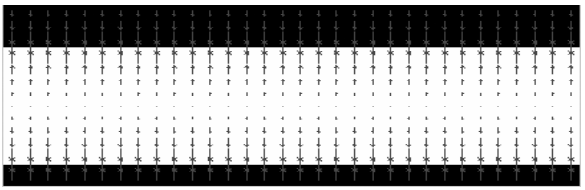

(b) Gradient vector flow without direction information

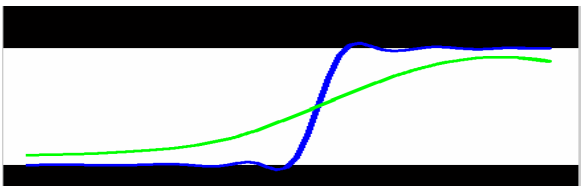

(c) Tracking results using GVF: the green curve is the initial curve and the blue curve is the final contour.

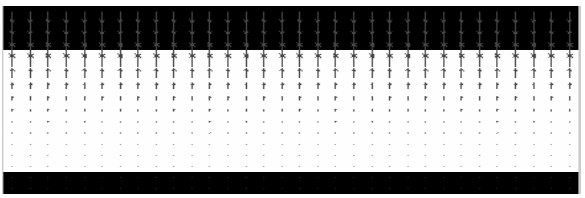

(d) Gradient vector flow with direction information

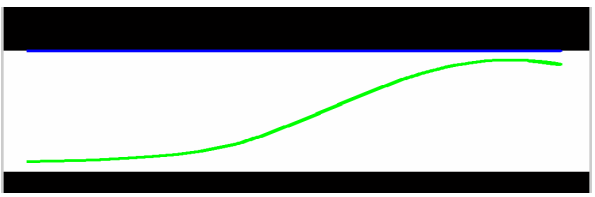

(e) Tracking results using DGVF: the blue line is the final contour and the initialization is the same as in (c)

Figure 2. Examples of boundary tracking using GVF and DGVF on a synthetic image.

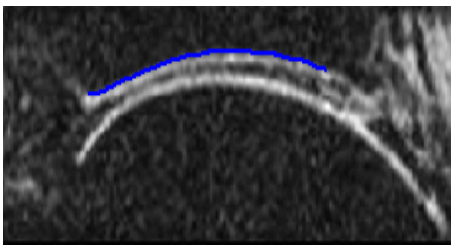

Figure 3. Example of tracking results using the DGVF snake.

3. EXPERIMENTAL RESULTS

Ground truth data are collected manually for comparison. The metric adopted in this paper for comparison is Pratt's quality measurement [6]:

$$FOM = \frac{\sum_{i=1}^{I_A} \frac{1}{1 + \alpha (d(i)^2)}}{\max(I_A, I_I)} \quad (16)$$

where I_A is the number of boundary pixels delineated by computer-aided segmentation method, I_I is the number of boundary pixels delineated by the technicians. $d(i)$ is the Euclidean distance between a boundary pixel delineated by the technicians and the nearest boundary pixel delineated by computer-aided segmentation and α is a scaling constant, with a suggested value of 1/9 [6]. A perfect match between the boundary pixels delineated by computer-aided segmentation method and the boundary pixels delineated by the technicians would yield F=1 in (16).

A cartilage sequence was used to compare the performance of the two snakes: traditional GVF snake and directional GVF snake (DGVF). Figure 4 shows the tracking results of the Tibial bone-cartilage interface, tibial cartilage surface, Talar cartilage surface and Talar bone-cartilage interface of the 11-th frame of the video sequence using DGVF respectively. The 7-th, 11-th, and 15-th frames of the sequence were selected to compute the FOM. The FOM values computed between the ground truth data and the results obtained by the automated methods are 0.8703, 0.8315, 0.7856 for the 7-th, 11-th, 15-th frames when the DGVF snake is used for tracking and 0.8432, 0.6665, 0.5442 for the 7-th, 11-th, 15-th frames when the traditional GVF snake is used for tracking. Thus the directional GVF snake provides higher FOM values compared to those of the standard GVF snake for this sequence. We also performed a subjective visual check of the tracking results using three MRI technicians and three studies. Each of the three technicians agreed that DGVF snake boundary was faithful to the actual boundary in all three studies and that the DGVF results improved upon those of GVF.

4. CONCLUSION

This paper studies ankle articular cartilage surface segmentation using the GVF snake. Because the cartilage is very thin, the traditional GVF snake is not suitable for accurate tracking of the cartilage surface, as a slight error in initialization will lead to tracking of the incorrect surface. Thus, we have developed a directional GVF snake for tracking the surface of the articular cartilage of the ankle. We have compared our algorithm with the traditional GVF snake, and experiments show that the DGVF snakes increases the FOM values yielded by the traditional GVF snake.

Accurate surface tracking is possible with the DGVF snake, and will allow us to use the tracking results obtained by our DGVF snake to construct a 3-D model of the articular cartilage which can be used to compute the thickness of the cartilage and the volume of the cartilage. Precise, reproducible measurements of these parameters will allow us to monitor changes in the articular cartilage typically seen in degenerative diseases such as post traumatic osteoarthritis of the ankle.

REFERENCES

[1] E. Yelin and L.F. Callahan, "The economic cost and social and psychological impact of musculoskeletal conditions," *Arthritis Rheum.*, vol. 38, pp. 1351-1362, 1995

[2] R. Burgkart, C. Glaser, S. Hinterwimmer, M. Hudelmaier, K.H. Englmeier, M. Reiser, F. Eckstein, "Feasibility of T and Z scores from magnetic resonance imaging data for quantification of cartilage loss in osteoarthritis," *Arthritis Rheum.*, vol. 48, pp. 2829-2835, 2003.

[3] F. Eckstein, H. Sittek, S. Milz, R. Putz, M. Reiser, "The morphology of articular cartilage assessed by magnetic resonance imaging (MRI): Reproducibility and anatomical correlation," *Surg. Radiol. Anat.*, vol. 16, pp. 429-438, 1994.

[4] M. Kass, A. Witkin and D. Terzopolous, "Snakes: Active contour models," *Int. Jour. Comput. Vis.*, vol. 1, pp. 321-331, 1987.

[5] C. Xu and J.L. Prince, "Snakes, shapes, and gradient vector flow," *IEEE Trans. Image Processing* vol. 7, pp. 359-369, 1998.

[6] W. K. Pratt, *Digital Image Processing*, (Wiley, New York, 1978), pp. 495-501.

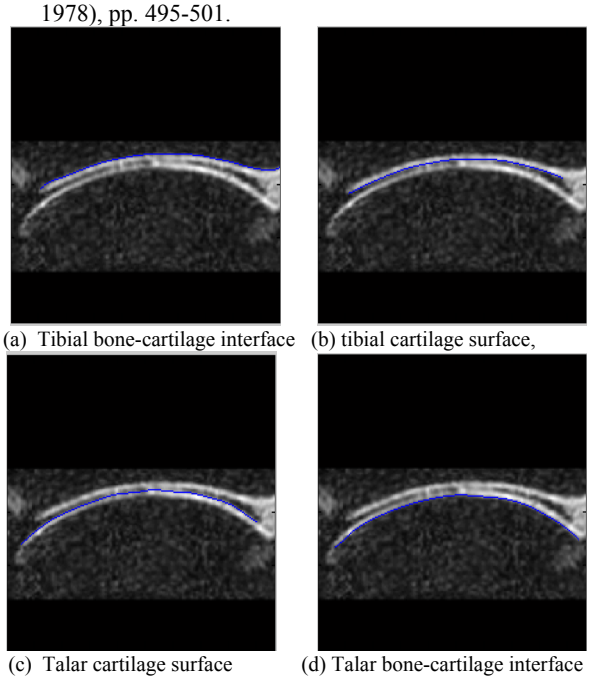

(a) Tibial bone-cartilage interface (b) tibial cartilage surface, (c) Talar cartilage surface (d) Talar bone-cartilage interface

Figure 4. An example of tracking results using DGVF snake.